

RSC Advances



This is an *Accepted Manuscript*, which has been through the Royal Society of Chemistry peer review process and has been accepted for publication.

Accepted Manuscripts are published online shortly after acceptance, before technical editing, formatting and proof reading. Using this free service, authors can make their results available to the community, in citable form, before we publish the edited article. This *Accepted Manuscript* will be replaced by the edited, formatted and paginated article as soon as this is available.

You can find more information about *Accepted Manuscripts* in the [Information for Authors](#).

Please note that technical editing may introduce minor changes to the text and/or graphics, which may alter content. The journal's standard [Terms & Conditions](#) and the [Ethical guidelines](#) still apply. In no event shall the Royal Society of Chemistry be held responsible for any errors or omissions in this *Accepted Manuscript* or any consequences arising from the use of any information it contains.

PAPER

Fabrication and property of low crystallinity nanofibrillar cellulose and nanofibrillar cellulose-graphene oxide composite

Cite this: DOI: 10.1039/x0xx00000x

Received 00th January 2015,

Accepted 00th January 2015

DOI: 10.1039/x0xx00000x

www.rsc.org/

Hongming Lou^{1,2}, Duming Zhu^{1,2}, Long Yuan^{1,2}, Houkeng Lin^{1,2}, Xuliang Lin^{1,2}, Xueqing Qiu^{*1,2}

Nanofibrillar cellulose with low crystallinity (LNC) was fabricated by adding water into cellulose solution, which was facile, efficient and environmentally friendly. Strong and translucent nanofibrillar cellulose film with low crystallinity (LNCF) was prepared from LNC suspension by filtration. Transmission electron microscopy showed that LNC was individually separated whiskers with a length of 200 nm, a width of 20 nm. Structure characterization of LNC showed that the main crystal form of LNC was cellulose II and the crystallinity was as low as 22.3 %. LNCF performed excellent optical transparency of 91.7 % when the thickness of the film was 40 μm . Tensile strength and young's modulus of LNCF reached 64.7 MPa and 3062.8 MPa respectively. Meanwhile, nanofibrillar cellulose-graphene oxide composite (LNC-GO) with layer by layer structure was obtained by mixing LNC with graphene oxide at the mass ratio of 1:1, and the tensile strength and young's modulus of LNC-GO were 84.3 MPa and 4406.2 MPa respectively.

Introduction

Cellulose, the most abundant natural polymer in the biosphere, is the main component of several natural fibers, such as flax, hemp, cotton, jute and sisal, occupying about one-third of plant composition.¹ It is a homopolysaccharide composed of β -1-4 glucopyranose units, and the degree of polymerization ranges from 10000 to 15000.² Each repeating unit of cellulose contains three hydroxyl (-OH) groups. These hydroxyl groups and their ability to form hydrogen bonds play a major role in directing the crystal packing and governing the physical properties of cellulose, including low density (1.6 g/cm^3), good mechanical properties and biodegradability.³ Nanocellulose mainly include nanocrystalline cellulose and nanofibrillar cellulose, which is classified according to the feature of morphology, preparation methods, function, etc.⁴ Nanofibrillar cellulose is mainly existed in the cell walls of plants, which presents it lots of special properties, such as high specific surface area, strong mechanical properties, etc.^{5,6} Compared with nanocrystalline cellulose, nanofibrillar cellulose is more flexible because of its stretch chains, which endows it a host of potential and fascinating application in the field of fine chemicals and composite materials by compounding it with other material.^{7,8}

Numerous manufacture technologies have been put forward to prepare nanofibrillar cellulose. Among the methods, the mechanical method using wood fibers as raw materials consisted of refining and high pressure homogenizing processes. However, such method tends either to damage the microfibril structure by reducing molar mass or fail to sufficiently disintegrate the fibers.⁹ Meanwhile, nanofibrillar cellulose were recently disintegrated with a more efficient process where 2,2,6,6-tetramethylpiperidine-1-oxyl (TEMPO) oxidation was utilized, which is toxic and lack

biocompatibility for such chemical method.¹⁰ The use of enzymatic pre-treatment may lower processing cost by decreasing the number of passes through the homogenizer, and has advantages from the environmental point of view when compared with chemical methods. However, the low yield of enzymatic pre-treatment severely restricts its application, which is only suitable for lab research.¹¹ Therefore, it is quiet meaningful to prepare nanofibrillar cellulose in a method of environmentally friendly and scalable.

Like the most nanomaterials, a crucial challenge in the processing of bulk-quantity nanofibrillar cellulose is to avoid the aggregation due to the strong hydrogen bonds in the intramolecular and intermolecular of cellulose,¹² which makes it difficult for a large number of hydroxyl groups reacting with other reagents. Meanwhile, in order to facilitate more hydroxyl groups exposed, which is essential to improve the availability and accessibility of cellulose, it is necessary to lower the crystallinity.¹³

In this work, nanofibrillar cellulose with low crystallinity (LNC) and nanofibrillar cellulose film (LNCF) was fabricated through the following steps, namely, dissolution of cellulose, precipitation of LNC by adding water and filtration of LNC suspension, which was facile and efficient. By means of Fourier transform infrared (FTIR) and X-ray diffraction (XRD), it was possible and efficient to analyze the structure and property of the obtained nanofibrillar cellulose. Meanwhile, the formation mechanism of nanofibrillar cellulose was revealed.

Graphene, a single-atom-thick sheet of carbon atoms arrayed in a honeycomb pattern, is the world's thinnest, strongest, and stiffest material, and its tensile strength and young's modulus were 125 GPa and 1000 GPa, respectively.¹⁴ Graphite oxide (GO) retained the excellent mechanical properties of graphene, and possessed several oxygen-containing functional groups, including epoxy, hydroxyl, carboxyl, which can contact with hydrogen bonding of LNC.

Composites of GO and LNC could improve the mechanical property of LNC significantly.

Materials and Methods

Materials

Commercially bleached bamboo dissolving pulp (BBP), with average length of 230 μm and average width of 13.25 μm , was used for the raw materials, kindly provided in dry form by Hunan Top Bamboo Industry Development Co., Ltd. (Yiyang, China). Other reagents of analytical grade used were: sodium hydroxide, urea, uranyl acetate, graphite powder, P_2O_5 , $\text{K}_2\text{S}_2\text{O}_8$, H_2SO_4 , (Guangdong Guanghua Co., Ltd, China).

Preparation of LNC, LNCF, GO and LNC-GO

The experimental schematic flow diagram illustrating preparation process of LNC suspension and LNCF was presented in Fig. 1. 1g BBP was added into 100 mL mixed solution of sodium hydroxide, urea and distilled water with a mass ratio of 7:12:81. The obtained BBP solution was cooled to $-10\text{ }^\circ\text{C}$, stirred for 5 min, and centrifuged at 10000 r/min for 3 min to remove the insoluble substance, then the cellulose solution was obtained. 150 mL distilled water was added into the cellulose solution by dropwise with sonication, then nanofibrillar cellulose with low crystallinity (LNC) was obtained. LNC suspension was filtrated using a Millipore hazardous filtration system (142-mm Millipore Hazardous Waste Filtration System, Millipore, Ireland) assisted with compressed air for 12 h. The obtained wet films were pressed with filtration membrane and blotter paper at 207 kPa for 3 min and at 345 kPa for another 3 min, dried at $60\text{ }^\circ\text{C}$ for 24 h, and then the nanofibrillar cellulose film with low crystallinity (LNCF) was fabricated.

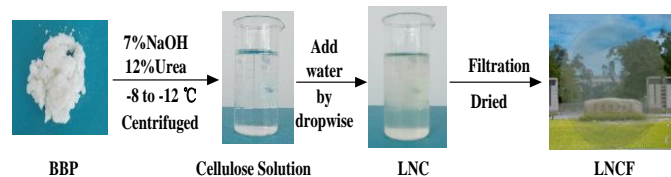


Fig. 1 Preparation process of LNC suspension and LNCF.

Graphite oxide was prepared with modified hummers method.¹⁵ Graphite powder (3 g), P_2O_5 (2.5 g), and $\text{K}_2\text{S}_2\text{O}_8$ (2.5 g) were mixed with 96 % wt H_2SO_4 (12 mL). The mixture was kept at $80\text{ }^\circ\text{C}$ overnight. The oxidized graphite was obtained by centrifugation to remove the un-oxidized graphite, washed for five times with water and one time with acetone, and dried at vacuum for 12 h. Subsequently, the oxidized graphite was added into 96 % wt H_2SO_4 (120 mL) with an ice bath for 3 h. Then KMnO_4 (15 g) was gradually added into the mixture within 1 h. The mixture was kept at $35\text{ }^\circ\text{C}$ for 2 h and diluted with 200 mL of ice water within 30 min. After the dilution, the mixture was magnetically stirred at room temperature for 2 h. Distilled water (400 mL) and 30 % wt H_2O_2 (50 mL) were added into the mixture to terminate the oxidation reaction. Then the obtained product was filtered and washed with 10 % wt HCl solution and consequently washed with water for 10 times, then dried under vacuum for 12 h, thus the graphite oxide was obtained. Subsequently, graphite oxide (0.04 g) was dispersed in 1000 mL distilled water with sonication for 30 min to fabricate graphene oxide suspension. LNC-GO was prepared by mixing LNC with graphene oxide suspension at a mass ratio of 1:1.

Morphology measurement

A drop of diluted LNC suspension (with solid consistency of 0.1%) was directly deposited onto copper grids (300 meshes) for 30 s, followed by maintaining on the grids for 10 min. Then the samples were rinsed with water and negatively stained with 0.5 % wt uranyl acetate.¹⁶ Images were observed on high transmission electron microscopy (TEM) at 160 kV (JMF-2100F, HITACHI Corp, Japan).

A drop of diluted LNC suspension (with solid consistency of 0.1%) was directly adhered to object stage and dried for 12h at room temperature. The obtained samples were sprayed with thin gold layer to improve the conductivity. Then the samples were recorded with conductive tapes on a scanning electron microscopy (ZEISS, Merlin) at 3.0 kV.

Characterization of structure and properties

The particle size distribution of LNC suspension was evaluated by dynamic light scattering using a Brookhaven Laser Light Scattering Spectrometer (IB-90Plus) with a scattering angle of 90 ° . The light source is a power solid state laser with a maximum power of 35 mW and a wavelength of 659 nm. 5 mL of LNC suspension was transferred into a polyester resin cuvette cell with a cap. Each sample was repeated five times and the mean value was accepted as the final particle size.

Wide-angle X-ray diffraction (XRD) analysis for LNCF was measured with Bruker D8 ADVANCE X-ray diffractometer equipped with Cu K α radiation generated at 40 kV and 40 mA. The LNCF was mounted in a special holder through which X-ray beam could pass centrally. Scattering radiation was detected in a 2θ range from 2 ° to 40 ° with a scanning rate of $5\text{ }^\circ/\text{min}$. The ratio of scattering intensity at 22.7 ° vs. intensity at 20.4 ° ($I_{22.7}/I_{20.4}$) was indicative of the ratio of Cellulose I and Cellulose II.¹⁷ The crystallinity index was calculated by the following equation: $\text{CrI} = (I_{002} - I_{\text{am}}) / I_{002} \times 100\%$ in accordance to the Segal method¹⁸, where I_{002} was the overall intensity of the peak at 2θ about 22.7 ° for Cellulose I and 20.4 ° for Cellulose II, respectively, and I_{am} was the minimum intensity of the baseline at 2θ about 18 ° . Each sample was repeated three times.

2 mg of dried BBP and LNC were mixed with 200 mg of spectroscopic grade KBr respectively. Fourier transform infrared (FTIR) of BBP and LNC were performed (Bruker Vector 33) between 4000 and 400 cm^{-1} . The FTIR spectrophotometer was equipped with an attenuated total reflectance (ATR) crystal. Each sample was scanned for 32 times.

Tensile tests of LNCF were conducted by a tensile tester (Instron 5564) equipped with 100 N load cells, according to ASTM D638-10.¹⁹ LNCF was cut into rectangular strips with a width and length of 15 and 60 mm respectively, and subsequently pre-conditioned at 50 % relative humidity and $23\text{ }^\circ\text{C}$ for 24 h. The speed of testing was set at a crosshead speed of 1 mm/min. At least five times were tested for each specimen. Tensile strength was calculated from the determined displacement and initial gage length.²⁰ Young's modulus was calculated as the slope of the stress-strain curve in the stress region of 30-70 MPa.²¹

UV spectrophotometer (Hitachi U-3010) was used to measure the spectral transparency of LNCF at a wavelength range from 400 to 800 nm. Circular specimen with radius of 5cm, and thickness of 40 μm were placed in a quartz cuvette. The specimens were pre-conditioned at 50 % relative humidity and $23\text{ }^\circ\text{C}$ for 24 h. and three tests were performed for each sample.

Results and discussion

Morphology of LNC

Decreasing the crystallinity of cellulose will facilitate more hydroxyl groups exposed to improve the availability and accessibility of cellulose, which is essential for better compounding it with other material to obtain composite with novel property. Nanofibrillar cellulose with low crystallinity was fabricated by dissolution of cellulose in NaOH/Urea solution at low temperature and then adding water into the cellulose solution to precipitate the nanofibrillar cellulose, as shown in the Fig. 1. With the aid of dynamic light scattering, Fourier transform infrared and X-ray diffraction, the structure and property of the obtained nanofibrillar cellulose was investigated.

The particle size distribution evaluated by dynamic light scattering is a relative value rather than an absolute value, which is suitable for measuring particle with low aspect ratio, such as spherical and ellipsoidal particle.²² Meanwhile, it could turn out to be assisted proofs to evaluate whether LNC was in nanosize level. The statistical distribution of LNC suspension was illustrated in Fig. 2. The average particle size of LNC was 3662.6 nm by intensity, 445.4 nm by volume, 23.1 nm by number. Since intensity is proportional to the sixth power of particle size, volume is proportional to the third power of particle size and number is proportional to particle size, so the average particle size could be reflected by number effectively.²³ In this study, the average particle size calculated by intensity was much larger than the average particle size calculated by volume and number, which was attributed to the polydispersity of LNC suspension. For LNC suspension, more than 90% was in a particle size range of 21.3~32.6 nm.

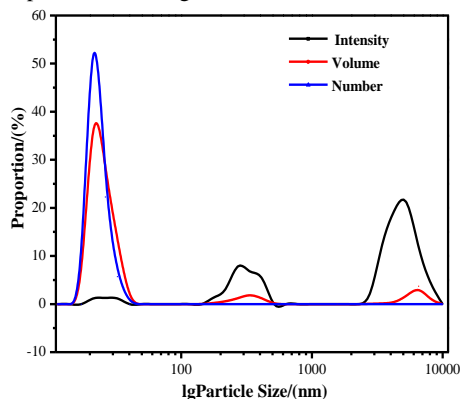


Fig. 2 Particle size distribution of LNC suspension

As illustrated in the Fig. 3 of TEM, the nanoparticles showed a bar shape, and LNC was individually separated whiskers with a length of 200 nm, a width of 20 nm. Therefore, it was worth noting that a significant portion of the fibers were converted to nano-scale fibers, which was in agreement with the results showed in particle size distribution.

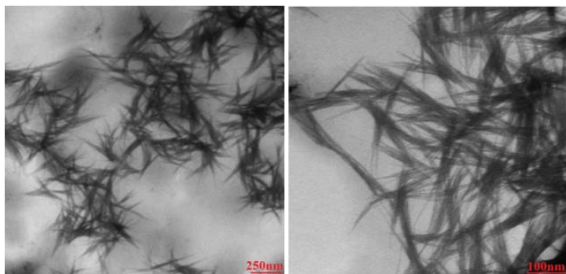


Fig. 3 TEM images of LNC.

Characterization of structure

The structure and crystallinity behaviour of BBP and LNC were performed by XRD. As illustrated in Fig. 4, it was clear that BBP mainly corresponded to Cellulose I crystal form and showed highest scattering intensity at 15.34° , 14.46° , 22.76° .²⁴ Meanwhile, the ratio of scattering intensity at 22.7° vs. intensity at 20.4° ($I_{22.7}/I_{20.4}$) was indicative of the ratio of Cellulose I and Cellulose II. The ratio of Cellulose I to Cellulose II crystal form was 3.45 for BBP. On the other hand, LNC showed three shape peaks observed at $2\theta = 11.95^\circ$, 20.05° , 22.17° , mainly corresponding to Cellulose II crystal form.²⁴ The ratio of Cellulose I to Cellulose II crystal form was 1.03 for LNC, which indicated that the structure of LNC was transformed into Cellulose II from Cellulose I at a high degree during the preparation process. The progressive decrease (from 3.45 to 1.03) of the ratio $I_{22.7}/I_{20.4}$ from BBP to LNC may be interpreted as a decrease in the proportion of cellulose I crystallites with respect to cellulose II crystallites. During the process of dissolution and regeneration, cellulose chains had a tendency to form Cellulose II, which was more thermodynamically stable.²⁵ Meanwhile, the crystallinity of LNC was 22.3 % according to the Segal method, which was significantly lower than the crystallinity of BBP (75.2%) and carbamate fibers, lyocell fibers, viscose fibers reported in references.^{26,27,28} The reason accounting for the crystallinity decreasing for LNC was the destruction of intramolecular and intermolecular hydrogen bonds during the dissolution process of BBP.²⁹

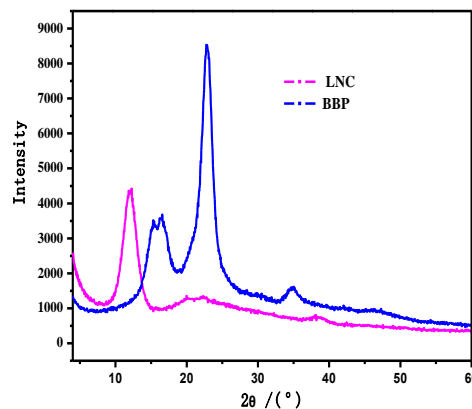


Fig. 4 XRD spectrum of BBP and LNC

FTIR spectroscopy was used to investigate the difference of the structure between BBP and LNC. As showed in Fig. 5, BBP and LNC showed a same FTIR spectrum, which indicated that there were no significant and obvious changes of chemical structure during the preparation of LNC. Meanwhile, the absorption intensity at 1429 cm^{-1} of cellulose was proportional to the crystallinity.³⁰ There was a peak at 1427 cm^{-1} in the spectrum of BBP, but no obvious peak of LNC, which revealed that the crystallinity of LNC was lower. As a result, it was in agreement with the result of XRD. The intramolecular hydrogen bonding of $\text{O}(2)\text{H} \cdots \text{O}(6)$ and $\text{O}(3)\text{H} \cdots \text{O}(5)$, and the intermolecular hydrogen bonding of $\text{O}(6)\text{H} \cdots \text{O}(3)$ in cellulose were generally shown at $3455\text{--}3410$, $3375\text{--}3340$, and $3310\text{--}3230\text{ cm}^{-1}$, respectively.³¹ For LNC, the maximum absorbance of the OH stretching vibration was shifted to 3348 cm^{-1} from 3329 cm^{-1} , showing the intramolecular hydrogen bonding of $\text{O}(3)\text{H} \cdots \text{O}(5)$ for Cellulose II crystal of LNC, which was attributed to the transformation related to the change of intramolecular bonds. Consequently, the crystal system of LNC was changed from cellulose I to cellulose II at a high degree.

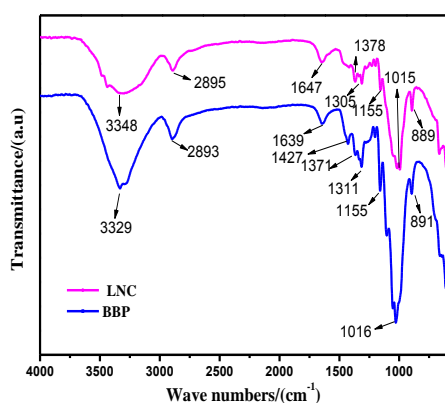


Fig. 5 FTIR spectrum of BBP and LNC

On the basis of the information obtained from TEM, XRD, and FTIR, a schematic process describing the preparation of LNC was presented in Fig. 6. When cellulose was immersed in the pre-cooled solvent, sodium hydroxide, urea hydrates, and free water can penetrate into the cellulose structure and destroy the intramolecular and intermolecular hydrogen bonds of the cellulose at a low temperature, which would lead to the salvation of cellulose chains.³² In our present work, the most proper amount of water added was control as 1.5 times of the cellulose solution in volume. When water was added, the concentration of sodium hydroxide and urea was lower, thus cellulose chains aggregated and precipitated slightly because water was a poor solvent for cellulose,³⁵ then LNC with low aggregation degree was obtained. LNCF was fabricated through filtration of LNC suspension, followed by pressing and drying. Subsequently, LNCF was prepared by mixed LNC suspension with graphene oxide suspension at a mass ratio of 1:1, followed by filtration, pressing and drying successively.

Characterization of properties

The visible light transmittance at 400-800nm wavelength for LNC and BBP was shown in Fig.7, it was worth noting that the thickness of LNC and BBP were same to eliminate the impact of thickness. As revealed in Fig. 7, LNCF showed excellent optical transparency in all visible wavelengths. When thickness of the film was 40 μm , the optical transparency of LNCF was 91.7 %, which was substantially higher than BBP. Meanwhile, nanofibrillar cellulose film prepared by mechanical process was 87.5 %.³⁴ In our present work, LNC of high optical transparency was obtained.

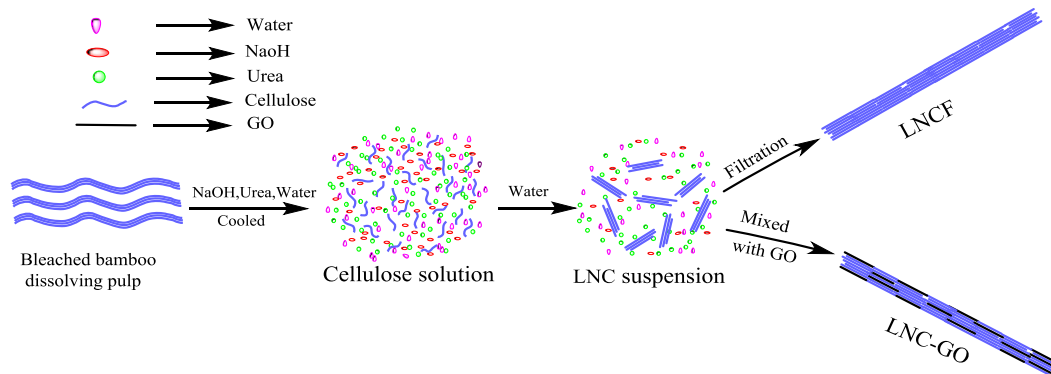


Fig. 6 Schematic preparation process of LNC, LNCF and LNC-GO

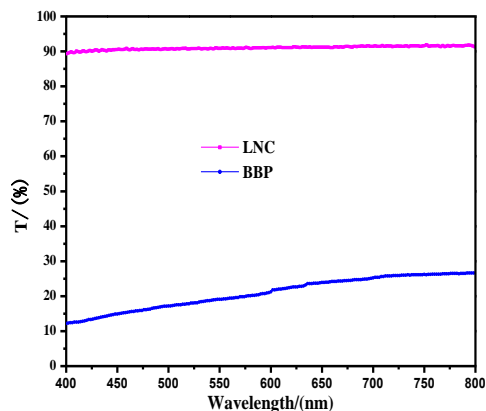


Fig. 7 UV spectrum of BBP and LNCF

Graphite oxide presented several oxygen-containing functional groups, including epoxy, hydroxyl, carboxyl, which would facilitate it compounding with the hydrogen bonding of LNC. SEM was used to evaluate the morphologies of LNC-GO. From Fig. 8 (a), plenty of flakes could be observed on the surface of LNC-GO, and the size of LNC-GO flake was about 1 μm , which was closed to the size of graphite oxide.³⁵ As illustrated in Fig. 8 (b), layer by layer structure of LNC-GO could be seen, which was similar with graphene oxide paper.³⁶ When graphene oxide suspension was added into cellulose solution, nanofibrillar cellulose precipitated out and graphene oxide was encapsulated in the nanofibrillar cellulose, then LNC-GO with layer by layer structure was obtained after filtration.

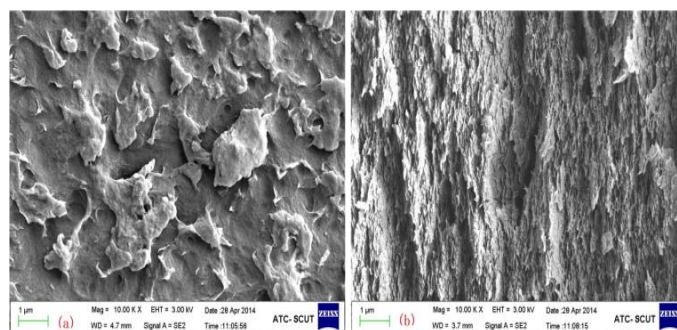


Fig. 8 (a) Surface morphology of LNC-GO
(b) Cross section morphology of LNC-GO

The stress-strain curves of tensile test of BBP and LNC was showed in Fig. 9. The tensile strength of the obtained LNC improved to 64.7 MPa from 23.5 MPa and young's modulus improved to 3062.8 MPa from 1472.4 MPa. Compared with BBP, bonding strength between cellulose chains of LNC improved because the contact areas and interactions between cellulose chains improved. Consequently, LNC showed excellent mechanical properties than BBP. As a reinforcing phase,³⁷ graphene oxide was compounded with LNC to improve the unique tensile strength of the composite. The tensile strength and young's modulus of LNC-GO increased to 84.3 MPa and 4406.2 MPa, respectively. As a result, GO performed a significant effect on the structure and property of LNC-GO.

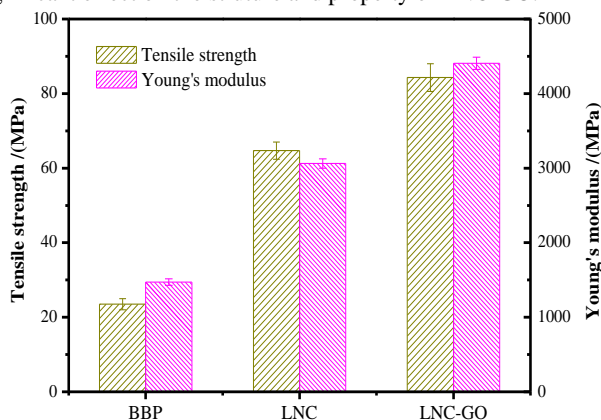


Fig. 9 Tensile strength and young's modulus of BBP, LNC and LNC-GO

Conclusions

This work developed a facile, efficient, and environmentally friendly method to prepare nanofibrillar cellulose, and consequently gives rise to new exciting possibilities regarding large-scale production of inexpensive cellulose-based material. From high transmission electron microscopy, LNC was individually separated whiskers with a length of 200 nm, a width of 20 nm, which was in agreement with the results illustrated in dynamic light scattering. Furthermore, XRD tests and FTIR spectra confirmed that the crystallinity of LNC was substantially lower than cellulose.

Subsequently, strong and optically transparent nanofibrillar cellulose film was prepared by filtration of LNC suspension. The optical transparency of the film was 91.7 % when thickness of the film is 40 μm , and the tensile strength and young's modulus of the film reached 64.7 MPa and 3062.8 MPa, respectively. Meanwhile, LNC-GO with layer by layer structure was obtained by compounding the LNC and GO, and the tensile strength and young's modulus of LNC-GO were 84.3 MPa and 4406.2 MPa, respectively. These composite materials will be potentially used in the field of ultrahigh-strength material.

Acknowledgements

The authors acknowledge the financial support of International S&T Cooperation Program of China (2013DFA41670), National Natural Science Foundation of China (21376100), Guangdong Province Science and Technology Plan (2013B051000011) and the Fundamental Research Funds for the Central Universities of China (2014ZG0022).

Notes and references

¹School of Chemistry and Chemical Engineering, South China University of Technology, Guangzhou, China.

²State Key Laboratory of Pulp and Paper Engineering, South China University of Technology, Guangzhou, China.

† BBP, Bleached bamboo dissolving pulp.

LNC, Nanofibrillar cellulose with low crystallinity.

LNCf, Nanofibrillar cellulose film with low crystallinity.

LNC-GO, Nanofibrillar cellulose-graphene oxide composite.

- M. Rosa, E. Medeiros, J. Malmonge, K. Gregorski, D. Wood, L. Mattoso, G. Glenn, W. Orts and S. Imam, *Carbohydrate Polymers*, 2010, **81**, 83-92.
- H. Jørgensen, J. B. Kristensen and C. Felby, *Biofuels, Bioproducts and Biorefining*, 2007, **1**, 119-134.
- S. Y. Lee, D. J. Mohan, I.-A. Kang, G.-H. Doh, S. Lee and S. O. Han, *Fibers and Polymers*, 2009, **10**, 77-82.
- H. Charreau, M. L. Foresti and A. Vázquez, *Recent patents on nanotechnology*, 2013, **7**, 56-80.
- K. Qiu and A. N. Netravali, *Polymer Reviews*, 2014, **54**, 598-626.
- L. T. Nguyen, S. Chen, N. K. Elumalai, M. P. Prabhakaran, Y. Zong, C. Vijila, S. I. Allakhverdiev and S. Ramakrishna, *Macromolecular Materials and Engineering*, 2013, **298**, 822-867.
- Siró and D. Plackett, *Cellulose*, 2010, **17**, 459-494.
- D. Klemm, F. Kramer, S. Moritz, T. Lindström, M. Ankerfors, D. Gray and A. Dorris, *Angewandte Chemie International Edition*, 2011, **50**, 5438-5466.
- J. Zhang, H. Song, L. Lin, J. Zhuang, C. Pang and S. Liu, *Biomass and Bioenergy*, 2012, **39**, 78-83.
- T. Saito, Y. Nishiyama, J. L. Putaux, M. Vignon and A. Isogai, *Biomacromolecules*, 2006, **7**, 1687-1691.
- M. Henriksson, G. Henriksson, L. Berglund and T. Lindström, *European Polymer Journal*, 2007, **43**, 3434-3441.
- K. L. Spence, R. A. Venditti, Y. Habibi, O. J. Rojas and J. J. Pawlak, *Bioresource technology*, 2010, **101**, 5961-5968.
- A. Pinkert, K. N. Marsh and S. Pang, *Industrial & Engineering Chemistry Research*, 2010, **49**, 11121-11130.
- A. K. Geim and K. S. Novoselov, *Nature materials*, 2007, **6**, 183-191.
- Y. Xu, H. Bai, G. Lu, C. Li and G. Shi, *Journal of the American Chemical Society*, 2008, **130**, 5856-5857.
- R. Lamed, E. Setter and E. Bayer, *Journal of Bacteriology*, 1983, **156**, 828-836.
- B. M. Cherian, A. L. Leão, S. F. de Souza, L. M. M. Costa, G. M. de Olyveira, M. Kottaisamy, E. Nagarajan and S. Thomas, *Carbohydrate Polymers*, 2011, **86**, 1790-1798.
- L. Segal, J. Creely, A. Martin and C. Conrad, *Textile Research Journal*, 1959, **29**, 786-794.
- A. Karmarkar, S. Chauhan, J. M. Modak and M. Chanda, *Composites Part A: Applied Science and Manufacturing*, 2007, **38**, 227-233.
- M. K. Kompella and J. Lambros, *Polymer Testing*, 2002, **21**, 523-530.
- A. Kelly and H. Lilholt, *Philosophical Magazine*, 1969, **20**, 311-328.
- J. Li, X. Wei, Q. Wang, J. Chen, G. Chang, L. Kong, J. Su and Y. Liu, *Carbohydrate polymers*, 2012, **90**, 1609-1613.
- S. K. Brar and M. Verma, *TrAC Trends in Analytical Chemistry*, 2011, **30**, 4-17.
- Y. Peng, D. J. Gardner, Y. Han, A. Kiziltas, Z. Cai and M. A.

- Tshabalala, *Cellulose*, 2013, **20**, 2379-2392.
25. A. C. O'SULLIVAN, *Cellulose*, 1997, **4**, 173-207.
 26. D. Klemm, B. Heublein, H. P. Fink and A. Bohn, *Angewandte Chemie International Edition*, 2005, **44**, 3358-3393.
 27. D. Bondeson, A. Mathew and K. Oksman, *Cellulose*, 2006, **13**, 171-180.
 28. S. Levis and P. Deasy, *International journal of pharmaceuticals*, 2001, **230**, 25-33
 29. K. Biradha, *CrystEngComm*, 2003, **5**, 374-384.
 30. R. T. O'Connor, E. F. DuPré and D. Mitcham, *Textile Research Journal*, 1958, **28**, 382-392.
 31. S. Y. Oh, D. I. Yoo, Y. Shin and G. Seo, *Carbohydrate Research*, 2005, **340**, 417-428.
 32. J. Cai and L. Zhang, *Macromolecular Bioscience*, 2005, **5**, 539-548.
 33. J. Cai, S. Kimura, M. Wada, S. Kuga and L. Zhang, *ChemSusChem*, 2008, **1**, 149-154.
 34. D. A. Dikin, S. Stankovich, E. J. Zimney, R. D. Piner, G. H. Dommett, G. Evmenenko, S. T. Nguyen and R. S. Ruoff, *Nature*, 2007, **448**, 457-460.
 35. Y. Xu, H. Bai, G. Lu, C. Li and G. Shi, *Journal of the American Chemical Society*, 2008, **130**, 5856-5857.
 36. X. Bai, C. Wan, Y. Zhang and Y. Zhai, *Carbon*, 2011, **49**, 1608-1613.
 37. G. Gonçalves, P. A. Marques, A. Barros-Timmons, I. Bdkin, M. K. Singh, N. Emami and J. Grácio, *Journal of Materials Chemistry*, 2010, **20**, 9927-9934.

Table of Contents Entry

Nanofibrillar cellulose of low crystallinity and nanofibrillar cellulose-graphene oxide composite of excellent properties were fabricated in a facile way.

